JBC Papers in Press. Published on September 14, 2015 as Manuscript M115.675769
The latest version is at http://www.jbc.org/cgi/doi/10.1074/jbc.M115.675769

Posttranslational Regulation of Human DNA Polymerase ι

Justyna McIntyre[1,2], Mary P. McLenigan[1], Ekaterina G. Frank[1], Xiaoxia Dai[3], Wei Yang[4], Yinsheng Wang[3] and Roger Woodgate[1,*]

[1] From the Laboratory of Genomic Integrity, National Institute of Child Health and Human Development, National Institutes of Health, Bethesda, MD 20892-3371, USA

[2] From the Institute of Biochemistry and Biophysics, Polish Academy of Sciences, ul. Pawinskiego 5a, 02-106 Warsaw, Poland

[3] From the Department of Chemistry, University of California Riverside, Riverside, CA 92521-0403, USA

[4] From the Laboratory of Molecular Biology, National Institute of Diabetes, Digestive, Kidney Diseases, National Institutes of Health, Bethesda, MD 20892, USA

Running Title: *Ubiquitination of polι*

To whom correspondence should be addressed: Roger Woodgate, Laboratory of Genomic Integrity, National Institute of Child Health and Human Development, National Institutes of Health, Bethesda, MD 20892-3371, USA. Tel.: +1-301-217-4040; Fax: Email: woodgate@nih.gov

Keywords: Y-family DNA polymerase, DNA polymerase ι, Post-translational modification, Ubiquitin, Translesion DNA Synthesis, DNA Repair, Mutagenesis

Background: Many proteins are subject to posttranslational regulation, such as ubiquitination.
Results: Human DNA polymerase ι (polι) can be monoubiquitinated at >27 unique sites and exposure to naphthoquinones results in polyubiquitination of polι.
Conclusion: Ubiquitination sites are located across the entire polι polypeptide, as well as various structural motifs.
Significance: Ubiquitination at these sites are likely to alter polι's cellular functions *in vivo*.

ABSTRACT

Human DNA polymerases (pols) η and ι are Y-family DNA polymerase paralogs that facilitate translesion synthesis (TLS) past damaged DNA. Both polη and polι can be monoubiquitinated *in vivo*. Polη has been shown to be ubiquitinated at one primary site. When this site is unavailable, three nearby lysines, may become ubiquitinated. In contrast, mass spectrometry analysis of monoubiquitinated polι revealed that it is ubiquitinated at over 27 unique sites. Many of these sites are localized in different functional domains of the protein, including the catalytic polymerase domain, the PCNA-interacting region, the Rev1-interacting region, as well as its Ubiquitin Binding Motifs, UBM1 and UBM2. Polι monoubiquitination remains unchanged after cells are exposed to DNA damaging agents such as UV-light (generating UV-photoproducts), ethyl methanesulfonate (generating alkylation damage), mitomycin C (generating interstrand crosslinks), or potassium bromate (generating direct oxidative DNA damage). However, when exposed to naphthoquinones, such as menadione and plumbagin, which cause indirect oxidative damage through mitochondrial dysfunction, polι becomes transiently polyubiquitinated via K11- and K48-linked chains of ubiquitin and subsequently

targeted for degradation. Polyubiquitination does not occur as a direct result of the perturbation of the redox cycle, as no polyubiquitination was observed after treatment with rotenone, or antimycin A, which inhibit mitochondrial electron transport. Interestingly, polyubiquitination was observed after the inhibition of the lysine acetyltransferase, KATB3/p300. We hypothesize that the formation of polyubiquitination chains attached to polι occurs via the interplay between lysine acetylation and ubiquitination of ubiquitin itself at K11- and K48- rather than oxidative damage *per se*.

INTRODUCTION

In order to survive the constant threat to their genomes from exposure to endogenous and exogenous DNA damaging agents, cells are equipped with an impressive array of DNA repair mechanisms. Yet situations arise where DNA lesions in the genome remain unrepaired and cells are forced to tolerate the DNA damage. One such tolerance mechanism is "translesion DNA synthesis" (TLS)[1]. During TLS, the high-fidelity replicase, which is unable to traverse the DNA lesion due to its constrained active site, is replaced with a specialized DNA polymerase (pol) with a more spacious active site that can accommodate the damaged DNA (1). Many of the DNA polymerases discovered in the past fifteen years appear to have some capacity to promote TLS. However, the best-characterized TLS polymerases belong to the Y-family of DNA polymerases (2). Y-family DNA polymerases are typified by human polη, which bypasses a thymine-thymine cyclobutane pyrimidine dimer efficiently and with much higher accuracy than any other human TLS polymerases (3). Because of their more spacious active sites (4), the TLS enzymes are also able to accommodate non-canonical Watson-Crick base pairing and are usually much more error-prone than high fidelity replicases when they replicate undamaged DNA (1). In specialized situations, such as during immunoglobulin somatic hypermutation, this creates genetic diversity and leads to high affinity antigen-specific immunoglobulins (5). However, under normal circumstances, random mutagenesis of chromosomal DNA is highly deleterious, often leading to mutagenesis and tumorigenesis in higher organisms.

It is clear, therefore, that the activity of the TLS polymerases needs to be tightly regulated, so that they only gain access to undamaged genomic DNA when appropriate. Previous studies have revealed that the post-translational modification of the TLS polymerases themselves, or their interacting partners, play a major role in regulating their cellular activities [reviewed in (6)]. In particular, both mono- and polyubiquitination appear to play a central role in regulating TLS polymerases since monoubiquitination of the proliferating cell nuclear antigen (PCNA) appears to control the switch between high fidelity replicases and TLS polymerases (7,8). PCNA can, however, be further polyubiquitinated. The addition of K63-linked polyubiquitin chains to PCNA that is monoubiquitinated at K164 leads to a damage avoidance template-switching pathway that in contrast to TLS allows for error-free DNA damage bypass (9,10).

In addition to PCNA, both human polη and polι TLS polymerases are also subject to monoubiquitination (11,12). Attaching a single ubiquitin moiety to one of four lysine residues in the C-terminus of polη blocks the physical interaction between polη and PCNA (12). As a consequence, polη needs to be actively de-ubiquitinated prior to interacting with PCNA and subsequently recruited to a stalled replication fork (12). The cellular role of polι monoubiquitination remains enigmatic. However, our previous results suggest that monoubiquitination of either polη or polι is a pre-requisite for the physical and functional interaction between the two polymerases (13).

Human polι is one of the least accurate DNA polymerases and exhibits a 10,000-fold range in base substitution fidelity depending on the template sequence copied [reviewed in (1)]. Polι has been extensively characterized at the biochemical level (14-19), and its *in vivo* re-localization in response to DNA damage has been shown (20,21). The enzyme is involved in the error-free bypass of methylglyoxal-induced minor groove lesions, N^2-carboxyethyl-2′-deoxyguanosine (22) and a deficiency in polι has

been suggested to cause sensitivity to oxidative and 4-hydroxynonenal DNA damage (23,24), as well as stimulate UV-induced mesenchymal carcinogenesis (25). However, the primary biological function of polι is still far from being understood.

Some assumptions on polι's cellular role can be derived from the various domains/motifs identified in polι. The N-terminal part of the protein contains two partly overlapping catalytic domains; a DNA polymerase domain and a dRP-lyase domain (26,27). The core polymerase domain is built of palm, finger, thumb, and little-finger sub-domains (28,29). The C-terminal portion of the protein is unstructured and devoted to facilitating interactions with a variety of proteins. Similar to other TLS polymerases, polι contains a PCNA interacting peptide motif responsible for the interaction with PCNA (30-32) and a Rev1 interacting region (33,34). It also contains two ubiquitin binding motifs (11).

Typically, the conjugation of ubiquitin to the lysine residue of a substrate protein occurs as a result of a three-enzyme cascade process involving ubiquitin-activating enzyme (E1), ubiquitin-conjugating enzyme (E2) and ubiquitin ligase (E3) (35)**.** Ubiquitin contains seven lysine residues (K6, K11, K27, K29, K33, K48 and K63) and is itself a target for further ubiquitination. Indeed, repetitive ubiquitination can establish polyubiquitin chains on a target protein. The length, the type of linkage, and consequent shape of conjugated polyubiquitin chains direct the function and processing of many intracellular proteins in eukaryotes [reviewed in (36)]. All types of ubiquitin chains exist in the cell; however, they vary in abundance and functionality. Different types of polyubiquitin chains regulate different biological processes by promoting proteasomal degradation, altering subcellular localization, modulating enzymatic activity and facilitating protein-protein interactions (37).

In the current work, we have used mass spectrometry analysis to identify the lysine residues that can be ubiquitinated in human polι. In contrast to PCNA, which is primarily ubiquitinated at K164 and polη, where the ubiquitinated residues are clustered in its C-terminus, the monoubiquitinated residues in polι are scattered amongst its various functional domains/motifs. Furthermore, unlike monoubiquitinated polη that is de-ubiquitinated upon UV-irradiation, the level of monoubiquitinated polι remains unchanged after exposure to UV, ethyl methanesulfonate, mitomycin C, or potassium bromate. Interestingly, however, after exposure to menadione and structurally related naphthoquinones polι is rapidly polyubiquitinated and intracellular levels of both the unmodified and the monoubiquitinated forms of polι decrease significantly. We present evidence that polι's polyubiquitination is not in response to oxidative DNA damage *per se*, but is rather due to the inhibition of KAT3B/p300 dependent acetylation of ubiquitin, which in turn, allows for the formation of K11- and K48-linked polyubiquitin chains on polι that subsequently target it for degradation.

Experimental Procedures

Reagents - 2,3 dimethoxy-1,4-naphthoquinone (DMNQ) was purchased from Enzo Life Sciences and ethyl methanesulfonate, mitomycin C, potassium bromate, menadione, 1,4-naphthoquinone, juglone, plumbagin, L002; rotenone, antimycin A were all purchased from Sigma-Aldrich.

Mammalian expression plasmids - Plasmid pJRM46, is a derivative of pCMV6AN-DDK (Origene) which expresses N-terminal FLAG-tagged full-length human polι (13). Derivatives with single or multiple K→A, or K→R substitutions were generated by chemically synthesizing appropriate DNA fragments (Genscript) that were subsequently cloned into pJRM46. Plasmid pRK7-POLI-3XFLAG, is a derivative of pRK7 (38), which expresses full-length human polι with three C-terminal FLAG-tags. The vector was constructed by inserting three tandem repeats of the FLAG epitope tag (DYKDDDDK) into the *Bam*HI and *Eco*RI sites of pRK7 to generate pRK7-3×FLAG. The full-length human *POLI* gene was amplified from HEK293T cells by reverse transcription PCR using primers POLI-S: AAAGCTAGCATGGAGAAGCTGGGGGTGGA, and POLI-AS:

AAAGGATCCTTTATGTCCAATGTGGAAATC T. These primers introduce 5' *Nhe*I and 3' *Bam*HI sites into the amplicon, which was and subcloned into the *Xba*I and *Bam*HI sites of the pRK7-3XFLAG vector. A full list of plasmids used in the current study is shown in Table 1.

Plasmid transfection, protein expression and Western blotting – HEK293T cells were plated onto 100 mm culture plates at a seeding density of 3 x 10^6 cells. When cells were ~40 percent confluent, plasmids were transfected into cells using Turbofectin 8.0 according to the manufacturer's instructions (Origene). Cells were either mock treated, or exposed to a variety of agents twenty-four or forty-eight hours after transfection depending upon the treatment times required. At appropriate times thereafter, cells were gently collected, washed twice with cold Dulbecco's PBS without calcium or magnesium, and suspended in modified RIPA buffer (25 mM Tris-HCl pH 7.6, 150 mM NaCl, 1% NP-40, 1 mM EDTA, 1 mM PMSF, 1 mM Na_3VO_4 and Sigma Protease Inhibitor Cocktail and lysed by sonication for 10 seconds. Immediately after sonication, the extracts were clarified by centrifugation at +4°C for 15 minutes in a Sorvall Biofuge Pico at 16,000g. The supernatants (extracts) were transferred to fresh tubes and protein concentrations were measured using the Pierce BCA Assay (Pierce Biotechnology). Cell extracts were kept at +4°C until being separated on a 4-16% gradient SDS PAGE gel. Proteins were transferred to a PVDF membrane and FLAG-tagged polι was visualized using Tropix Western-Star chemiluminescent kit using mouse anti-FLAG monoclonal antibodies (Abnova) followed by secondary anti-mouse antibody (Novagen). Where noted, other antibodies were used as followed: POLI monoclonal antibody (M01), clone 8G9 (Abnova), or polyclonal rabbit antibodies raised against a KLH-conjugated peptide corresponding to the C-terminal 15 amino acid residues of polι (20). Where noted, the level of polι was compared to β-actin present in the extracts, and were visualized using rabbit anti-β-actin antibodies (Cell Signaling Technologies). The intensity of the individual bands was quantified using the ImageJ 1.47 application (NIH, USA).

Mass spectrometry analysis - Purified recombinant N-terminal FLAG-tagged human polι was purchased from Origene Technologies (Rockville, MD) and was supplied at a final concentration of 0.106 mg/ml. Roughly 80% of the total protein represents unmodified FLAG-polι and ~10% represents a slower-migrating modified FLAG-polι (Fig. 1A). A total of 5 μg of the combined FLAG-polι preparation was applied to a 1 mm thick precast 10% polyacrylamide NuPage gel (Life Technologies). Proteins were separated by SDS-PAGE by running the gel at 190 V for 3.75 hours. All subsequent solutions were prepared using ultrapure HPLC water. The gel was lightly stained using the Novex Collodial Blue Staining Kit (Life Technologies), in brand new disposable plastic trays. Unmodified and modified FLAG-polι bands were excised using a brand new hard-backed razor blade under water. Gel fragments were washed 2X with 50% acetonitrile in ultrapure water. Samples were sent to the Harvard Microchemistry Department (Harvard University, MA), where they were analyzed by mass spectrometry as a custom contract service.

pRK7-POLI-3XFLAG (1.5 μg) was transfected into HEK293T cells (70-80% confluence in a 6-well plate) using Lipofectamine 2000 (Invitrogen). After a 48-hour incubation, the C-terminal 3XFLAG-tagged polι protein was isolated and purified using anti-FLAG M2 beads (Sigma). The purified protein was digested with trypsin (Roche) at an enzyme/substrate ratio of 1:50, and subjected to LC-MS/MS analysis.

LC-MS/MS experiments were performed as described previously (39). Briefly, the peptides were separated on an EASY-nLC II and analyzed on an LTQ Orbitrap Velos mass spectrometer equipped with a nanoelectrospray ionization source (Thermo). The trapping column (150 μm × 50 mm) and separation column (75 μm × 120 mm) were packed with ReproSil-Pur C18-AQ resin (3 μm in particle size, Dr. Maisch HPLC GmbH, Germany). The peptide samples were firstly loaded onto the trapping column in CH_3CN/H_2O (2:98, v/v) at a flow rate of 4.0 μl/min, and resolved on the separation column with a 120-min linear gradient of 2-40% acetonitrile in 0.1%

formic acid and at a flow rate of 300 nl/min. The LTQ-Orbitrap Velos mass spectrometer was operated in the positive-ion mode, and the spray voltage was 1.8 kV. The full-scan mass spectra (*m*/*z* 300-2000) were acquired with a resolution of 60,000 at *m*/*z* 400 after accumulation to a target value of 500,000 in the linear ion trap. MS/MS data were obtained in a data-dependent scan mode where one full MS scan was followed with 20 MS/MS scans.

Results

Sites of ubiquitination in polι - It has been previously reported that polι is monoubiquitinated *in vivo* (11). However, at the time that we embarked on these studies, the location of the modified residue(s) had yet to be determined. To identify the site(s) of ubiquitination in polι we initially utilized the contract services of the Harvard Microchemistry Department (Harvard University) to provide mass spectrometry analysis of a commercially available preparation of N-terminal FLAG-tagged human polι (Origene) (Fig. 1A). The preparation contains a significant amount of a slower migrating protein that cross-reacts with anti-FLAG antibodies, as well as both polyclonal and monoclonal antibodies against polι (Fig.1B). Based upon the earlier work of Bienko *et al*. (11), we hypothesized that the slower migrating band was likely to be monoubiquitinated polι.

Mass spectrometry analysis of the isolated slower-migrating FLAG-polι protein indicated it was indeed monoubiquitinated polι, which was modified at six unique lysine residues (K248, K522, K526, K530, K549 and K704). Although we had limited mass spectrometry coverage of the very C-terminus of polι, we rationalized that the C-terminal K715 residue might also be subject to ubiquitination, since it is most probably localized on the surface of the protein and thus likely to be exposed to ubiquitinating enzymes.

To determine which of the residues might be the primary site of polι ubiquitination, we transfected human HEK293T cells with a series of recombinant plasmids carrying FLAG-tagged polι each containing a single lysine to alanine substitution (K248A, K522A, K526A, K530A, K549A, K704A and K715A) and checked the extent of polι ubiquitination by western blotting and probing with anti-FLAG antibodies. Remarkably most of the polι mutants were ubiquitinated at levels comparable to the wild-type protein (Fig. 2A). Interestingly, the largest reduction in ubiquitination occurred in the K715A mutant, which exhibited approximately 60% of the level observed with the wild-type protein, indicating that K715 is indeed a target for ubiquitination. Based on these observations, it appears that none of the seven lysines is an exclusive site of ubiquitination. However, we rationalized that modification at lysines in close proximity to the respective alanine substitution, might mask the effect of individual lysine mutations (e.g., K522, K526 and K530). To test this hypothesis, we determined the extent of ubiquitination of polι mutants containing multiple K→A substitutions. This included double (K704A/K715A), quadruple (K522A/ K526A/ K530A/ K549A), and even septuple (K248A/ K522A/ K526A/ K530A/ K549A/ K704A/ K715A) substitutions (Fig. 2B). To our surprise, ubiquitination of polι in the septuple mutant was only diminished by ~50% compared to the wild-type protein suggesting the existence of additional ubiquitination sites in polι. By analogy to polη, where a K682A substitution leads to ubiquitination at nearby lysine residues (12), we made K→A substitutions at polι residues K237, K245 and K550. Based on the results obtained by Wagner *et al*. (40), who reported proteome-wide analysis of *in vivo* ubiquitination sites, we also made K→A substitutions at K267 and K271. However, a duodecuple mutant carrying all 12K→A substitutions did not prevent monoubiquitination of polι (Fig. 2B), thereby implying additional sites of ubiquitination in polι.

We therefore undertook an independent mass spectrometry analysis approach, this time using C-terminal FLAG-tagged polι. Interestingly, we identified six ubiquitination sites in polι that were clustered in the N-terminal half of the polymerase (K53, K283, K309, K271, K310 and K320). None of these sites emerged in the original analysis of N-terminal FLAG tagged polι performed at the Harvard Microchemistry department and only one residue (K271), was

identified in the earlier studies by Wagner *et al.* (40).

Thus, by three independent approaches, two specifically focused on polι (described herein) and one proteome-wide (Wagner *et al.*), seventeen independent ubiquitination sites in polι were identified. We were interested in determining if substitutions at these sites would finally block ubiquitination of polι. Given the close structural proximity of polι K51 and K72 residues to K53 (29), we also made substitutions at these residues. The combined mutant has 19K→A substitutions. We noted that this mutant has altered gel electrophoretic mobility (Fig. 3A) and decided to limit the influence of the multiple alanine substitutions on the global charge of the protein and consequently its structure, so we also generated a 19K→R mutant.

Interestingly, the 19K→A mutant showed 60% higher levels of polι ubiquitination than the 19K→R mutant (Fig. 3), suggesting that multiple K→A mutations probably changed the structure of polι and possibly exposed lysine residues that perhaps would not normally be subject to monoubiquitination. We also observed the same effect when comparing the 12K→A to the 12K→R mutants. In light of the fact that the K→R changes in the combined polι mutants reduced ubiquitination of polι more acutely than the K→A mutations, we decided to re-evaluate the effect of a single K715R substitution, since the K715A mutant gave the greatest reduction in the levels of ubiquitination (Fig. 2). Again, the conservative K715R substitution diminished ubiquitination of polι to a greater extent than K715A. In some regards, this is surprising, since one might expect that the extreme C-terminal residue would be exposed and there would not be a large structural effect of the alanine, or arginine substitutions.

Recent technical progress in mass spectrometry-based methods in combination with novel ubiquitin enrichment strategies using di-Gly-lysine specific antibody (41) have significantly increased the number of documented ubiquitinated proteins and pinpointed many of their ubiquitin-modified lysines on a global level, including many TLS proteins (6). Within the last four years, several groups have reported large-scale detection of lysine ubiquitination events in human cells and in nine of these studies ubiquitination sites of polι have been identified (41-49).

Figure 4 summarizes all the lysine residues in polι that have been shown to be ubiquitinated. In total, 27 lysine residues of polι have been experimentally shown to be ubiquitinated. Based upon structural considerations, we have identified another three lysine residues that could potentially be ubiquitinated. Eight of the sites were detected just once. The remaining 19 ubiquitination sites in polι were identified in anywhere between 2 to 6 independent studies, often using very different experimental strategies (e.g., ectopically expressed vs. chromosomally expressed polι and/or different detection methods). However, no single site has been identified in all of the PTM studies. Thus, unlike polη, which is ubiquitinated at one primary site and a handful of secondary sites (12), polι does not appear to possess a primary site for ubiquitination, but is, instead, ubiquitinated at multiple lysine residues.

Polι ubiquitination in response to a variety of DNA damaging agents - The 30 potential ubiquitination sites are distributed along the entire length of the polι peptide. However, some are clustered in domains and motifs of polι that are important for its cellular function in DNA damage tolerance (dRP lyase domain, catalytic polymerase domain, PIP, RIR, UBM1 and UBM2) (Fig. 4). We were therefore interested in determining if the ubiquitination status of polι is influenced by exposure to DNA damaging agents. Indeed, there is a precedent for damage-induced de-ubiquitination of human polη, so as to allow it to interact with ubiquitinated PCNA and facilitate TLS (12). We therefore examined polι ubiquitination in response to treatment with agents that cause different types of DNA damage such as UV irradiation which results in both cyclobutane pyrimidine dimers and 6-4 photoproducts; ethyl methanesulfonate which generates alkylation damage (50); mitomycin C which generates interstrand crosslinks (51,52); and two oxidizing agents, potassium bromate and menadione (53,54). Somewhat surprisingly, most of the DNA damaging agents did not result in any significant change in the extent of polι ubiquitination, even

several hours after the initial treatment (Fig. 5A-D). In contrast, in cells treated with 30 μM menadione for one hour (time 0), we observed an increase of polι with much slower mobility, that is consistent with polyubiquitination of polι (Fig. 5E). Furthermore, the intracellular levels of polι decrease significantly 3-5 hours after treatment, suggesting that the posttranslationally modified polι protein is targeted for degradation.

Polι ubiquitination in response to treatment with various naphthoquinones and inhibitors of mitochondrial function - Our observation that potassium bromate did not elicit the same polyubiquitination of polι as menadione, suggests that polyubiquitination of polι is unlikely to occur as a result of oxidative damage *per se*, but occurs in specific response to menadione treatment. While both agents cause oxidative DNA damage, they do so by different mechanisms. For example, potassium bromate induces glutathione-mediated oxidative base damage (53), whereas menadione does so by inducing mitochondrial dysfunction, leading to an increase in reactive oxygen species (ROS) (54). However, we observed no significant increase in polι polyubiquitination after inhibition of the mitochondrial respiratory chain complex I with rotenone (55), or antimycin A, which inhibits cytochrome C reductase and the production of ATP (56) (Fig. 6), indicating that simple mitochondrial dysfunction is not the root cause for polι polyubiquitination.

In contrast, we discovered that polι polyubiquitination occurs after exposure to naphthoquinones that are structurally related to menadione (Fig. 7), including 1,4-naphthoquinone, juglone and plumbagin. Similar to menadione, all three compounds stimulated polι polyubiquitination in a concentration-dependent manner (Fig. 7). A particularly strong effect was observed after exposure to low concentrations of juglone and plumbagin (Fig. 7C & D). However, another naphthoquinone, 2,3 dimethoxy-1,4-naphthoquinone (DMNQ) that also causes significant oxidative DNA damage (57) did not induce polι polyubiquitination (Fig. 8). Although the UV-induced ubiquitination/deubiquitination of polη and polι seem to be differentially regulated (c.f., (12) and Fig 5A), pol η also appears to undergo polyubiquitination in response to menadione, and plumbagin treatment (unpublished observations). Whether this occurs as a result of a common pathway controlling the polyubiquitination of both polymerases in response to naphthoquinones remains to be determined.

Polι ubiquitination in response to treatment with an inhibitor of KAT3B/p300 - It is apparent that the effects of menadione, juglone, 1,4 naphthoquinone and plumbagin cannot be simply attributed to oxidative DNA damage, or mitochondrial dysfunction. However, naphthoquinones are also known to inhibit the activity of the lysine acetyltransferase KAT3B/p300 (58,59). We therefore considered the possibility that the inhibition of ubiquitin acetylation may promote the polyubiquitination of polι. To test this hypothesis, HEK293T cells were treated with the KAT3B/p300 inhibitor, L002. Indeed, similar to the effects of naphthoquinones, L002 results in the polyubiquitination of polι (Fig. 7E).

Mass spectrometry analysis of polyubiquitinated forms of polι - To further explore the nature of polyubiquitinated forms of polι appearing after treatment with naphthoquinones, we performed mass spectrometry analysis on the purified ubiquitin-conjugated polι. To do so, we used M2 anti-FLAG beads (Sigma) to pull-down N-terminal FLAG-tagged polι expressed in HEK293T cells that had been treated for 1 hour with 30 μM menadione (Fig. 7A), followed by tryptic digestion and LC-MS/MS analysis. This analysis was repeated twice, with independently prepared extracts and extracts from non-treated cells were used as controls. In control experiments, we predominantly observed monoubiquitinated forms of polι. In these extracts, we identified 7 ubiquitinated lysines (K87, K271, K283, K309, K486, K488 and K508). All of them except K508 were known as potential ubiquitination sites from previous approaches. Interestingly, in extracts prepared from menadione-treated cells, where intensive polyubiquitination of polι was observed, we identified four ubiquitinated lysines (K271, K309, K320 and K488) located in the N-terminal and central part of polι. Three of them, K271, K309 and K488, were identified in both independent

experiments. Since all four residues were previously indicated in our earlier experiments, or in proteome-wide experiments (40,42,43,46,47), as potential ubiquitination sites in untreated cells, we conclude that menadione treatment most probably causes polyubiquitination of polι at lysine residues that are already monoubiquitinated, rather than *de novo* at novel lysines.

In polyubiquitin chains, ubiquitins are linked to each other via an isopeptide bond between the C-terminal glycine of one ubiquitin and one of the lysine residues of the next ubiquitin. Ubiquitin contains seven lysine residues (K6, K11, K27, K29, K33, K48 and K63) and all of them can become ubiquitinated to establish polyubiquitin chains of different shape and biological function [reviewed in (36)]. Mass spectrometry analysis of polyubiquitinated polι revealed that the polyubiquitin chains formed in response to menadione are formed via K11- and K48-linkages (Fig. 9B & 9C). Aside from these two peptides carrying a diglycine remnant, we also observed unmodified tryptic peptides derived from ubiquitin, including TLSDYNIQK (amino acid residues 55-63) and TITLEVEPSDTIENVK (amino acids residues 12-27). Moreover, we observed K11- and K48- linkages in polyubiquitinated polι obtained from plumbagin treated cells (unpublished observations). Presumably these linkages are formed in response to a common signal induced by exposure to naphthoquinones.

K48-linked polyubiquitin chains represent one of the most known and abundant ubiquitin linkages in the cell and target marked proteins to degradation by the 26S proteasome (60,61). The cellular role of the K11-linkage is less known, however the function of homogenous K11-linked polyubiquitin chains are also implicated in proteasomal degradation (62,63). Consistent with the notion that polyubiquitinated polι is subject to proteasomal degradation, we observed an increase in the background levels of polyubiquitinated polι in undamaged cells in the presence of the proteasome inhibitor, MG132 (Fig. 10).

Discussion

Ubiquitination is an important factor allowing for quick, controlled and reversible modification of a protein's fate, cellular abundance, function, localization, and the promotion of protein-protein interactions. Several proteins employed in TLS are known to be ubiquitinated *in vivo* and the protein modification is used to adjust the specificity of TLS mechanisms in a variety of ways [reviewed in (6)].

It has been a decade since the discovery that human polι can be monoubiquitinated *in vivo* (11), yet the consequences of the modification remains enigmatic. Our previous studies, which show the dependence of a polι-polη interaction on the ubiquitination of either protein (13) provides some early insights into a possible role of polι modification.

In the present study, we have identified a number of lysine residues in polι that can be covalently linked to ubiquitin. Unlike polη, which is ubiquitinated at one primary site and a handful of secondary sites (6,12), we discovered that polι is ubiquitinated at more than 27 unique sites (Fig. 4). Two thirds of the identified sites were detected in multiple autonomous studies using different experimental strategies (e.g., ectopic expression of N- and C-terminal FLAG tagged polι vs. native untagged chromosomally expressed polι and different methods of identification). While we cannot exclude the possibility that polι is ubiquitinated at random sites, we believe that the detection of specific ubiquitination sites in multiple independent studies increases the probability that those sites are likely to play key roles in regulating the cellular activities of polι.

When assayed by SDS-PAGE, the predominant form of polι is a single mono-ubiquitinated species, rather than multiply mono-ubiquitinated forms of polι. We note that under certain conditions, such as when cells are exposed to menadione, we do observe a "laddering" of FLAG-tagged polι, indicative of multiple monoubiquitination events (Fig. 7), but we cannot distinguish between the possibility of multiple monoubiquitinations of polι, or a single monoubiquitination event that is subsequently converted into a polyubiquitin chain. Our observations therefore indicate that once polι is monoubiquitinated at one particular site, it subsequently precludes monoubiquitination at additional sites in polι. Clearly, this is an area of

research that needs to be studied in detail and will be the subject of future studies.

No single K→A, or K→R substitution completely blocked monoubiquitination of polι. However a K→R substitution at K715 which is located at the very C-terminus of polι and which has been shown to be ubiquitinated in two independent proteome-wide approaches (43,49), gave the greatest reduction in monoubiquitination (Fig. 3). We predict that the structure of covalently-linked ubiquitin to K715 will position the ubiquitin moiety for a productive interaction with the UBM2 of polι (Fig. 11E). Similarly, ubiquitination at K522 may also facilitate an interaction between ubiquitin and UBM1 of polι (Fig. 11D). We hypothesize that such interactions may, in turn, help promote an interaction between polι and polη (13).

In contrast, monoubiquitination of other lysine residues may have a detrimental effect on polι's cellular functions. For example, many sites are located in the catalytic domain of the polymerase and may alter both DNA binding properties and polymerase activity of polι (Fig. 4, 11A and Table 2). Ubiquitination sites were also identified in both the PIP-box (PCNA-interacting region) and the RIR motif (Rev1-interacting region) and it seems highly unlikely that polι would be able to physically interact with either PCNA, or Rev1, if these sites are ubiquitinated (Fig. 11B & 11C).

Unlike polη, which is de-ubiquitinated upon UV-irradiation (12), the level of polι monoubiquitination remained constant after exposure to a variety of DNA damaging agents including UV-light, EMS, MMC, or the oxidative DNA damage inducers, potassium bromate (Fig. 5), rotenone and antimycin A (Fig. 6) and DMNQ, (Fig. 8). In dramatic contrast, menadione and several structurally related naphthoquinones, resulted in the rapid polyubiquitination of polι. Mass spectrometry of polyubiquitinated polι purified from menadione- and plumbagin-treated cells indicated that the polyubiquitin chains were formed through K11- and K48- linkages. Conjugation of ubiquitin via K48-linkage is well known to serve as a signal for proteasomal degradation (60,61). Indeed, the disappearance of polι 3-5 hours after exposure to menadione (Fig. 5E) is consistent with its degradation.

We initially considered that the signal triggering polyubiquitination of polι might be oxidative DNA damage, but this was rapidly excluded when we failed to observe polyubiquitination in response to potassium bromate (Fig. 5C), DMNQ (Fig. 8), rotenone, or antimycin A (Fig. 6). However, in addition to the induction of reactive oxygen species, the naphthoquinones are also known to exert a wide range of cellular effects leading to stress signaling, anti-angiogenesis and thiolate arylation of proteins and amines (64-66). One property of interest is their ability to inhibit the lysine acetyltransferase (KAT), p300 (58,59). All of the naphthoquinones (1,4-naphthoquinone, menadione, juglone, plumbagin) that induce polι polyubiquitination have previously been reported to inhibit the KAT activity of p300 (59). It is unknown whether DMNQ (which did not cause polι polyubiquitination), can inhibit the KAT activity of p300. However, since DMNQ lacks the critical hydroxyl group at the 5th position of the benzene ring that is required for inhibition of KAT activity (59) and the 2nd and 3rd positions that are normally subject to nucleophilic attack are occupied by methoxy groups (Fig. 8), we assume that it probably does not inhibit KAT activity,

It is now well established that acetylation is a key regulator of diverse biological processes, from metabolism to signaling and immunity (67). Indeed, like many proteins, ubiquitin is subject to acetylation (49,68). Interestingly, both K11- and K48- are moderately sensitive to acetylation (49,68). Thus, we hypothesize that if K11- and K48- of ubiquitin are acetylated, it would preclude the formation of polyubiquitin chains via these linkages. Our observation that the p300 inhibitor, L002, also induces polyubiquitination of polι strongly suggests that there is a competition between ubiquitination and acetylation at overlapping lysine residues in polι. We believe that such competition constitutes a novel mechanism to regulate the stability of polι that warrants further investigation.

CONFLICT OF INTEREST

The authors declare that they have no conflicts of interest with the contents of this article.

Author contributions– J.M. constructed all of the pJRM expression plasmids shown in Table 1, as well as designed, performed and analyzed the experiments shown in Figures 2, 3 and 4 and wrote the paper. M.P.M. performed and analyzed the experiments shown in Figures 1, 5, 6, 7, 8 and 10. E.G.F. prepared purified N-terminal FLAG-tagged polι for mass spectrometry analysis shown in Figure 4. X.D. and Y.W. designed, performed and analyzed the mass spectrometry experiments shown in Figure 4 and 9. W.Y. analyzed the structural ramifications of polι monoubiquitination shown in Figure 11 and Table 2. R.W. conceived and coordinated the study and wrote the paper. All authors reviewed the results and approved the final version of the manuscript.

REFERENCES

1. Sale, J. E., Lehmann, A. R., and Woodgate, R. (2012) Y-family DNA polymerases and their role in tolerance of cellular DNA damage. *Nat. Rev. Mol. Cell. Biol.* **13**, 141-152

2. Ohmori, H., Friedberg, E. C., Fuchs, R. P. P., Goodman, M. F., Hanaoka, F., Hinkle, D., Kunkel, T. A., Lawrence, C. W., Livneh, Z., Nohmi, T., Prakash, L., Prakash, S., Todo, T., Walker, G. C., Wang, Z., and Woodgate, R. (2001) The Y-family of DNA polymerases. *Mol. Cell* **8**, 7-8

3. Matsuda, T., Bebenek, K., Masutani, C., Hanaoka, F., and Kunkel, T. A. (2000) Low fidelity DNA synthesis by human DNA polymerase-η. *Nature* **404**, 1011-1013

4. Yang, W., and Woodgate, R. (2007) What a difference a decade makes: insights into translesion DNA synthesis. *Proc. Natl. Acad. Sci. U.S.A.* **104**, 15591-15598

5. Neuberger, M. S., and Rada, C. (2007) Somatic hypermutation: activation-induced deaminase for C/G followed by polymerase η for A/T. *J. Exp. Med.* **204**, 7-10

6. McIntyre, J., and Woodgate, R. (2015) Regulation of translesion DNA synthesis: Posttranslational modification of lysine residues in key proteins. *DNA Repair* **29**, 166-179

7. Hoege, C., Pfander, B., Moldovan, G. L., Pyrowolakis, G., and Jentsch, S. (2002) RAD6-dependent DNA repair is linked to modification of PCNA by ubiquitin and SUMO. *Nature* **419**, 135-141

8. Kannouche, P. L., Wing, J., and Lehmann, A. R. (2004) Interaction of human DNA polymerase η with monoubiquitinated PCNA; a possible mechanism for the polymerase switch in response to DNA damage. *Mol. Cell* **14**, 491-500

9. Motegi, A., Liaw, H. J., Lee, K. Y., Roest, H. P., Maas, A., Wu, X., Moinova, H., Markowitz, S. D., Ding, H., Hoeijmakers, J. H., and Myung, K. (2008) Polyubiquitination of proliferating cell nuclear antigen by HLTF and SHPRH prevents genomic instability from stalled replication forks. *Proc. Natl. Acad. Sci. U.S.A.* **105**, 12411-12416

10. Unk, I., Hajdu, I., Fatyol, K., Hurwitz, J., Yoon, J. H., Prakash, L., Prakash, S., and Haracska, L. (2008) Human HLTF functions as a ubiquitin ligase for proliferating cell nuclear antigen polyubiquitination. *Proc. Natl. Acad. Sci. U.S.A* **105**, 3768-3773

11. Bienko, M., Green, C. M., Crosetto, N., Rudolf, F., Zapart, G., Coull, B., Kannouche, P., Wider, G., Peter, M., Lehmann, A. R., Hofmann, K., and Dikic, I. (2005) Ubiquitin-binding domains in Y-family polymerases regulate translesion synthesis. *Science* **310**, 1821-1824

12. Bienko, M., Green, C. M., Sabbioneda, S., Crosetto, N., Matic, I., Hibbert, R. G., Begovic, T., Niimi, A., Mann, M., Lehmann, A. R., and Dikic, I. (2010) Regulation of translesion synthesis DNA polymerase η by monoubiquitination. *Mol. Cell* **37**, 396-407

13. McIntyre, J., Vidal, A. E., McLenigan, M. P., Bomar, M. G., Curti, E., McDonald, J. P., Plosky, B. S., Ohashi, E., and Woodgate, R. (2013) Ubiquitin mediates the physical and functional interaction between human DNA polymerases η and ι. *Nucleic Acids Res.* **41**, 1649-1660

14. Tissier, A., McDonald, J. P., Frank, E. G., and Woodgate, R. (2000) polι, a remarkably error-prone human DNA polymerase. *Genes & Dev.* **14**, 1642-1650

15. Zhang, Y., Yuan, F., Wu, X., and Wang, Z. (2000) Preferential incorporation of G opposite template T by the low-fidelity human DNA polymerase ι. *Mol. Cell. Biol.* **20**, 7099-7108

16. Frank, E. G., Sayer, J. M., Kroth, H., Ohashi, E., Ohmori, H., Jerina, D. M., and Woodgate, R. (2002) Translesion replication of benzo[*a*]pyrene and benzo[*c*]phenanthrene diolexpoxide adducts of deoxyadenosine and deoxyguanosine by human DNA polymerase ι. *Nucleic Acids Res.* **30**, 5284-5292

17. Frank, E. G., and Woodgate, R. (2007) Increased catalytic activity and altered fidelity of DNA polymerase ι in the presence of manganese. *J. Biol. Chem.* **282**, 24689-24696

18. Pence, M. G., Blans, P., Zink, C. N., Hollis, T., Fishbein, J. C., and Perrino, F. W. (2009) Lesion bypass of N^2-ethylguanine by human DNA polymerase ι. *J. Biol. Chem.* **284**, 1732-1740

19. Washington, M. T., Johnson, R. E., Prakash, L., and Prakash, S. (2004) Human DNA polymerase ι utilizes different nucleotide incorporation mechanisms dependent upon the template base. *Mol. Cell. Biol.* **24**, 936-943

20. Kannouche, P., Fernández de Henestrosa, A. R., Coull, B., Vidal, A., Gray, C., Zicha, D., Woodgate, R., and Lehmann, A. R. (2002) Localisation of DNA polymerases η and ι to the replication machinery is tightly co-ordinated in human cells. *EMBO J.* **21**, 6246-6256

21. Sabbioneda, S., Gourdin, A. M., Green, C. M., Zotter, A., Giglia-Mari, G., Houtsmuller, A., Vermeulen, W., and Lehmann, A. R. (2008) Effect of proliferating cell nuclear antigen ubiquitination and chromatin structure on the dynamic properties of the Y-family DNA polymerases. *Mol. Biol. Cell.* **19**, 5193-5202

22. Yuan, B., You, C., Andersen, N., Jiang, Y., Moriya, M., O'Connor, T. R., and Wang, Y. (2011) The roles of DNA polymerases κ and ι in the error-free bypass of N^2-carboxyalkyl-2'-deoxyguanosine lesions in mammalian cells. *J. Biol. Chem.* **286**, 17503-17511

23. Petta, T. B., Nakajima, S., Zlatanou, A., Despras, E., Couve-Privat, S., Ishchenko, A., Sarasin, A., Yasui, A., and Kannouche, P. (2008) Human DNA polymerase iota protects cells against oxidative stress. *EMBO J.* **27**, 2883-2895

24. Temviriyanukul, P., Meijers, M., van Hees-Stuivenberg, S., Boei, J. J., Delbos, F., Ohmori, H., de Wind, N., and Jansen, J. G. (2012) Different sets of translesion synthesis DNA polymerases protect from genome instability induced by distinct food-derived genotoxins. *Toxicol. Sci.* **127**, 130-138

25. Kanao, R., Yokoi, M., Ohkumo, T., Sakurai, Y., Dotsu, K., Kura, S., Nakatsu, Y., Tsuzuki, T., Masutani, C., and Hanaoka, F. (2015) UV-induced mutations in epidermal cells of mice defective in DNA polymerase η and/or ι. *DNA Repair* **29**, 139-146

26. Bebenek, K., Tissier, A., Frank, E. G., McDonald, J. P., Prasad, R., Wilson, S. H., Woodgate, R., and Kunkel, T. A. (2001) 5'-Deoxyribose phosphate lyase activity of human DNA polymerase ι in vitro. *Science* **291**, 2156-2159

27. Prasad, R., Bebenek, K., Hou, E., Shock, D. D., Beard, W. A., Woodgate, R., Kunkel, T. A., and Wilson, S. H. (2003) Localization of the deoxyribose phosphate lyase active site in human DNA polymerase ι by controlled proteolysis. *J. Biol. Chem.* **278**, 29649-29654

28. Nair, D. T., Johnson, R. E., Prakash, S., Prakash, L., and Aggarwal, A. K. (2004) Replication by human DNA polymerase ι occurs by Hoogsteen base-pairing. *Nature* **430**, 377-380

29. Kirouac, K. N., and Ling, H. (2009) Structural basis of error-prone replication and stalling at a thymine base by human DNA polymerase ι. *EMBO J.* **28**, 1644-1654

30. Vidal, A. E., Kannouche, P., Podust, V. N., Yang, W., Lehmann, A. R., and Woodgate, R. (2004) Proliferating cell nuclear antigen-dependent coordination of the biological functions of human DNA polymerase ι. *J. Biol. Chem.* **279**, 48360-48368

31. Haracska, L., Acharya, N., Unk, I., Johnson, R. E., Hurwitz, J., Prakash, L., and Prakash, S. (2005) A single domain in human DNA polymerase ι mediates interaction with PCNA: implications for translesion DNA synthesis. *Mol. Cell. Biol.* **25**, 1183-1190

32. Hishiki, A., Hashimoto, H., Hanafusa, T., Kamei, K., Ohashi, E., Shimizu, T., Ohmori, H., and Sato, M. (2009) Structural basis for novel interactions between human translesion synthesis polymerases and proliferating cell nuclear antigen. *J. Biol. Chem.* **284**, 10552-10560

33. Ohashi, E., Hanafusa, T., Kamei, K., Song, I., Tomida, J., Hashimoto, H., Vaziri, C., and Ohmori, H. (2009) Identification of a novel REV1-interacting motif necessary for DNA polymerase κ function. *Genes Cells* **14**, 101-111

34. Tissier, A., Kannouche, P., Reck, M. P., Lehmann, A. R., Fuchs, R. P., and Cordonnier, A. (2004) Co-localization in replication foci and interaction of human Y-family members, DNA polymerase polη and REVl protein. *DNA Repair* **3**, 1503-1514

35. Hershko, A., and Ciechanover, A. (1998) The ubiquitin system. *Annu. Rev. Biochem.* **67**, 425-479

36. Komander, D., and Rape, M. (2012) The ubiquitin code. *Ann. Rev. Biochem.* **81**, 203-229

37. Xu, P., Duong, D. M., Seyfried, N. T., Cheng, D., Xie, Y., Robert, J., Rush, J., Hochstrasser, M., Finley, D., and Peng, J. (2009) Quantitative proteomics reveals the function of unconventional ubiquitin chains in proteasomal degradation. *Cell* **137**, 133-145

38. Chen, T., Muratore, T. L., Schaner-Tooley, C. E., Shabanowitz, J., Hunt, D. F., and Macara, I. G. (2007) N-terminal α-methylation of RCC1 is necessary for stable chromatin association and normal mitosis. *Nat. Cell. Biol.* **9**, 596-603

39. Dai, X., Otake, K., You, C., Cai, Q., Wang, Z., Masumoto, H., and Wang, Y. (2013) Identification of novel α-n-methylation of CENP-B that regulates its binding to the centromeric DNA. *J. Proteome Re.s* **12**, 4167-4175

40. Wagner, S. A., Beli, P., Weinert, B. T., Nielsen, M. L., Cox, J., Mann, M., and Choudhary, C. (2011) A proteome-wide, quantitative survey of in vivo ubiquitylation sites reveals widespread regulatory roles. *Mol. Cell. Proteomics* **10**

41. Xu, G., Paige, J. S., and Jaffrey, S. R. (2010) Global analysis of lysine ubiquitination by ubiquitin remnant immunoaffinity profiling. *Nat. Biotech.* **28**, 868-873

42. Danielsen, J. M., Sylvestersen, K. B., Bekker-Jensen, S., Szklarczyk, D., Poulsen, J. W., Horn, H., Jensen, L. J., Mailand, N., and Nielsen, M. L. (2011) Mass spectrometric analysis of lysine ubiquitylation reveals promiscuity at site level. *Mol. Cell. Proteomics* **10**, M110 003590

43. Kim, W., Bennett, E. J., Huttlin, E. L., Guo, A., Li, J., Possemato, A., Sowa, M. E., Rad, R., Rush, J., Comb, M. J., Harper, J. W., and Gygi, S. P. (2011) Systematic and quantitative assessment of the ubiquitin-modified proteome. *Mol.Cell* **44**, 325-340

44. Povlsen, L. K., Beli, P., Wagner, S. A., Poulsen, S. L., Sylvestersen, K. B., Poulsen, J. W., Nielsen, M. L., Bekker-Jensen, S., Mailand, N., and Choudhary, C. (2012) Systems-wide analysis of ubiquitylation dynamics reveals a key role for PAF15 ubiquitylation in DNA-damage bypass. *Nat. Cell. Biol.* **14**, 1089-1098

45. Udeshi, N. D., Svinkina, T., Mertins, P., Kuhn, E., Mani, D. R., Qiao, J. W., and Carr, S. A. (2012) Refined preparation and use of anti-diglycine remnant (K-epsilon-GG) antibody enables routine quantification of 10,000s of ubiquitination sites in single proteomics experiments. *Mol. Cell. Proteomics* **12**, 825-831

46. Udeshi, N. D., Mertins, P., Svinkina, T., and Carr, S. A. (2013) Large-scale identification of ubiquitination sites by mass spectrometry. *Nat.Prot.* **8**, 1950-1960

47. Sarraf, S. A., Raman, M., Guarani-Pereira, V., Sowa, M. E., Huttlin, E. L., Gygi, S. P., and Harper, J. W. (2013) Landscape of the PARKIN-dependent ubiquitylome in response to mitochondrial depolarization. *Nature* **496**, 372-376

48. Mertins, P., Qiao, J. W., Patel, J., Udeshi, N. D., Clauser, K. R., Mani, D. R., Burgess, M. W., Gillette, M. A., Jaffe, J. D., and Carr, S. A. (2013) Integrated proteomic analysis of post-translational modifications by serial enrichment. *Nat. Meth.* **10**, 634-637

49. Hornbeck, P. V., Zhang, B., Murray, B., Kornhauser, J. M., Latham, V., and Skrzypek, E. (2015) PhosphoSitePlus, 2014: mutations, PTMs and recalibrations. *Nucleic Acids Res.* **43**, D512-520

50. Sega, G. A. (1984) A review of the genetic effects of ethyl methanesulfonate. *Mutat. Res.* **134**, 113-142

51. Warren, A. J., Maccubbin, A. E., and Hamilton, J. W. (1998) Detection of mitomycin C-DNA adducts in vivo by ^{32}P-postlabeling: time course for formation and removal of adducts and biochemical modulation. *Cancer Res.* **58**, 453-461

52. Li, L., Peterson, C. A., Lu, X., Wei, P., and Legerski, R. J. (1999) Interstrand cross-links induce DNA synthesis in damaged and undamaged plasmids in mammalian cell extracts. *Mol. Cell. Biol.* **19**, 5619-5630

53. Ballmaier, D., and Epe, B. (1995) Oxidative DNA damage induced by potassium bromate under cell-free conditions and in mammalian cells. *Carcinogenesis* **16**, 335-342

54. Criddle, D. N., Gillies, S., Baumgartner-Wilson, H. K., Jaffar, M., Chinje, E. C., Passmore, S., Chvanov, M., Barrow, S., Gerasimenko, O. V., Tepikin, A. V., Sutton, R., and Petersen, O. H. (2006) Menadione-induced reactive oxygen species generation via redox cycling promotes apoptosis of murine pancreatic acinar cells. *J. Biol. Chem.* **281**, 40485-40492

55. Li, N., Ragheb, K., Lawler, G., Sturgis, J., Rajwa, B., Melendez, J. A., and Robinson, J. P. (2003) Mitochondrial complex I inhibitor rotenone induces apoptosis through enhancing mitochondrial reactive oxygen species production. *J. Biol. Chem.* **278**, 8516-8525

56. Park, W. H., Han, Y. W., Kim, S. H., and Kim, S. Z. (2007) An ROS generator, antimycin A, inhibits the growth of HeLa cells via apoptosis. *J. Cell. Biochem.* **102**, 98-109

57. Seung, S. A., Lee, J. Y., Lee, M. Y., Park, J. S., and Chung, J. H. (1998) The relative importance of oxidative stress versus arylation in the mechanism of quinone-induced cytotoxicity to platelets. *Chem. Biol. Interact.* **113**, 133-144

58. Ravindra, K. C., Selvi, B. R., Arif, M., Reddy, B. A., Thanuja, G. R., Agrawal, S., Pradhan, S. K., Nagashayana, N., Dasgupta, D., and Kundu, T. K. (2009) Inhibition of lysine acetyltransferase KAT3B/p300 activity by a naturally occurring hydroxynaphthoquinone, plumbagin. *J. Biol. Chem.* **284**, 24453-24464

59. Vasudevarao, M. D., Mizar, P., Kumari, S., Mandal, S., Siddhanta, S., Swamy, M. M., Kaypee, S., Kodihalli, R. C., Banerjee, A., Naryana, C., Dasgupta, D., and Kundu, T. K. (2014) Naphthoquinone-mediated inhibition of lysine acetyltransferase KAT3B/p300, basis for non-toxic inhibitor synthesis. *J. Biol. Chem.* **289**, 7702-7717

60. Hofmann, R. M., and Pickart, C. M. (2001) *In vitro* assembly and recognition of Lys-63 polyubiquitin chains. *J. Biol. Chem.* **276**, 27936-27943

61. Welchman, R. L., Gordon, C., and Mayer, R. J. (2005) Ubiquitin and ubiquitin-like proteins as multifunctional signals. *Nature reviews. Mol. Cell. Biol.* **6**, 599-609

62. Jin, L., Williamson, A., Banerjee, S., Philipp, I., and Rape, M. (2008) Mechanism of ubiquitin-chain formation by the human anaphase-promoting complex. *Cell* **133**, 653-665

63. Matsumoto, M. L., Wickliffe, K. E., Dong, K. C., Yu, C., Bosanac, I., Bustos, D., Phu, L., Kirkpatrick, D. S., Hymowitz, S. G., Rape, M., Kelley, R. F., and Dixit, V. M. (2010) K11-linked polyubiquitination in cell cycle control revealed by a K11 linkage-specific antibody. *Mol. Cell* **39**, 477-484

64. Klaus, V., Hartmann, T., Gambini, J., Graf, P., Stahl, W., Hartwig, A., and Klotz, L. O. (2010) 1,4-Naphthoquinones as inducers of oxidative damage and stress signaling in HaCaT human keratinocytes. *Arch. Biochem. Biophys.* **496**, 93-100

65. Kayashima, T., Mori, M., Yoshida, H., Mizushina, Y., and Matsubara, K. (2009) 1,4-Naphthoquinone is a potent inhibitor of human cancer cell growth and angiogenesis. *Cancer Lett.* **278**, 34-40

66. Matsubara, K., Kayashima, T., Mori, M., Yoshida, H., and Mizushina, Y. (2008) Inhibitory effects of vitamin K3 on DNA polymerase and angiogenesis. *Int. J .Mol. Med.* **22**, 381-387

67. Caron, C., Boyault, C., and Khochbin, S. (2005) Regulatory cross-talk between lysine acetylation and ubiquitination: role in the control of protein stability. *BioEssays* **27**, 408-415

68. Jabusch, J. R., and Deutsch, H. F. (1985) Localization of lysines acetylated in ubiquitin reacted with p-nitrophenyl acetate. *Arch. Biochem. Biophys.* **238**, 170-177

69. Hishiki, A., Hashimoto, H., Hanafusa, T., Kamei, K., Ohashi, E., Shimizu, T., Ohmori, H., and Sato, M. (2009) Structural basis for novel interactions between human translesion synthesis polymerases and proliferating cell nuclear antigen. *J. Biol. Chem.* **284**, 10552-10560

70. Burschowsky, D., Rudolf, F., Rabut, G., Herrmann, T., Peter, M., and Wider, G. (2011) Structural analysis of the conserved ubiquitin-binding motifs (UBMs) of the translesion polymerase ι in complex with ubiquitin. *J. Biol. Chem.* **286**, 1364-1373

71. Cui, G., Benirschke, R. C., Tuan, H. F., Juranic, N., Macura, S., Botuyan, M. V., and Mer, G. (2010) Structural basis of ubiquitin recognition by translesion synthesis DNA polymerase ι. *Biochem.* **49**, 10198-10207

FOOTNOTE

Funding for this work was provided by the National Institute of Child Health and Human Development/National Institutes of Health Intramural Research Program (to R.W.); National Institute of Diabetes and Digestive and Kidney Diseases/National Institutes of Health Intramural Research Program (to W.Y.); the Foundation for Polish Science HOMING PLUS/2013-7/10 (to J.M.), and the National Institutes of Health (R01 DK082779 to Y.W.).

[1] The abbreviations used are: TLS, translesion DNA synthesis; pol, DNA polymerase; PCNA, proliferating cell nuclear antigen; PIP, PCNA interacting peptide motif; RIR, Rev1 interacting region; UBMs, ubiquitin binding motifs; PTM, posttranslational modification; EMS, ethyl methanesulfonate; MMC, mitomycin C; DMNQ, 2,3 dimethoxy-1,4-naphthoquinone

FIGURE LEGENDS

FIGURE 1. **Highly purified polι protein, purchased from Origene Technologies.** *A,* Commassie Brilliant Blue stained gel of FLAG-tagged polι purified from HEK293T cells. *B,* Western blot of purified polι. Polι was visualized using monoclonal antibodies to the FLAG epitope (track 1); polyclonal antibodies to polι (track 2); or monoclonal antibodies to polι (track 3). The images clearly show that the major band observed in the Coomassie Brilliant Blue stained gel corresponds to native FLAG-polι. The slower migrating band also contains polι and appears to be a posttranslationally modified form of polι. The faster migrating band observed in panel A, does not appear to be related to FLAG-polι since it does not cross-react to either the FLAG or polι antibodies.

FIGURE 2. **Effects of K→A substitutions on the extent of polι ubiquitination in HEK293T cells.** *A,* Single amino acid substitutions. *B,* Multiple amino acid substitutions. 2K, (K704A/ K715A); 4K, (K522A/ K526A/K530A/ K549A); 7K (K248A/ K522A/ K526A/ K530A/ K549A/ K704A/ K715A); 12K, (K237A/ K245A/ K248A/ K267A/ K271A/ K522A/ K526A/ K530A/ K549A/ K550A/ K704A/ K715A). Upper panel; a representative western blot using monoclonal anti-FLAG antibodies. Lower panel; densitometric quantification of polι monoubiquitination. Data are the mean values from six (A) or three (B) independent experiments, ±SD.

FIGURE 3. **Effects of K→A and K→R substitutions on the extent of ubiquitination of polι in HEK293T cells.** *A,* Western blot using monoclonal anti-FLAG antibodies. *B,* Lower panel; densitometric quantification of polι monoubiquitination. Data are the mean values from four to five independent experiments, ±SD. Lysine residues were changed to either alanine or arginine. 19K; (K51/ K53/ K72/ K237/ K245/ K248/ K267A/ K271A/ K283/ K309/ K310/ K320/ K522/ K526/ K530/ K549/ K550/ K704/ K715); 12K, (K237/ K245/ K248/ K267/ K271/ K522/ K526/ K530/ K549/ K550/ K704/ K715); and the C-terminal K715 residue.

FIGURE 4. **Sites of ubiquitination in polι. Lysine residues in polι that have been shown to be subject to ubiquitination are indicated with a colored dot.** The reference for each residue is given below the primary amino acid sequence of polι. As noted, polι can be ubiquitinated at more than 27 unique lysine residues. Some residues have been observed in multiple studies, but no single residue has been identified in every study. The various motifs and domains in polι are identified by color-coded bars above the primary amino acid sequence.

FIGURE 5. **Effect of DNA damaging agents on the extent of polι ubiquitination in HEK293T cells.** *A,* UV-irradiation (resulting in cyclobutane pyrimidine dimers and 6-4 photoproducts); *B,* EMS (resulting in alkylation DNA damage); *C,* MMC (resulting in interstrand crosslinks); *D,* Potassium bromate (resulting in oxidative DNA damage) **E**, Menadione (believed to cause oxidative damage and a variety of other cellular effects). Polι was visualized in western blots using monoclonal antibodies to the N-terminal FLAG epitope. The major band is unmodified polι, followed by mono-ubiquitinated polι. Slower migrating proteins are believed to be polyubiquitinated forms of polι.

FIGURE 6. **Effect of rotenone or antimycin A on polι ubiquitination in HEK293T cells.** Cells were treated with the indicated amount of either rotenone, or antimycin A for 1 hr prior to harvesting. Polι was visualized in western blots using monoclonal antibodies to the N-terminal FLAG epitope. The major band is unmodified polι, followed by mono-ubiquitinated polι. Under these conditions, there was no significant induction of polyubiquitinated polι.

FIGURE 7. **Effect of various naphthoquinones and a lysine acetyltransferase inhibitor, L002, on the extent of polι polyubiquitination in HEK293T cells.** Cells were treated for 1 hr with the indicated concentration of each compound. *A,* menadione; *B,* 1,4 naphthoquinone; *C,* juglone; *D,* plumbagin; *E,* L002. Polι was visualized in western blots using monoclonal antibodies to the N-terminal FLAG epitope. All compounds lead to an increase in polyubiquitinated forms of polι, with the most dramatic effects observed with the naturally occurring naphthoquinone, plumbagin. The chemical structures of each compound are shown on the right-hand side of each panel.

FIGURE 8. **Comparison of menadione, or DMNQ treatment on polι ubiquitination in HEK293T cells.** Cells were treated with the indicated amount of either mendione, or DMNQ for 1 hr prior to harvesting. Polι was visualized in western blots using monoclonal antibodies to the N-terminal FLAG epitope. The panel depicting polι ubiquitination after menadione treatment is a slightly darker exposure of Fig. 7A, so as to highlight the laddering of the ubiquitinated forms of polι (as noted by arrowheads). Under these conditions, there was no significant induction of polyubiquitinated polι after treatment with DMNQ.

FIGURE 9. **Mass spectrometry analysis of ubiquitinated polι recovered from menadione–treated HEK293T cells**. *A,* Western blot of purified proteins recovered from untreated and menadione–treated cells. Note that the menadione-treated cell extract contains significantly more polyubiquitinated forms of polι than the untreated cell extract. Both extracts were subjected to mass spectrometry analysis. *B,* The MS/MS of the $[M+2H]^{2+}$ ion of the peptide $_{43}$LIFAGKubiQLEDGR$_{54}$ from menadione-treated polι samples showing the K48-linkage of ubiquitin. *C,* The MS/MS of the $[M+2H]^{2+}$ ion of the peptide $_{7}$TLTGKubiTITLEVEPSDTIENVK$_{27}$ from menadione-treated polι samples showing the K11-linkage of ubiquitin. 'ubi', ubiqutination.

FIGURE 10. **Effect of the proteasomal inhibitor MG132, on polι ubiquitination in HEK293T cells.** Cells were either untreated, or exposed to the proteasomal inhibitor, MG132, for the times indicated. Polι was visualized in western blots using monoclonal antibodies to the N-terminal FLAG epitope. In both cases, the major band is unmodified polι, followed by monoubiquitinated polι. We note that the intensity of polyubiquitinated polι increases over time, in the MG132 treated cells compared to untreated cells, suggesting that the basal level of polyubiquitinated polι is normally kept to a minimum by 26S proteasomal degradation.

FIGURE 11. **Diagram of ubiquitinated lysine residues in the three-dimensional structures of human polι.** *A,* The catalytic domain of human polι (1-420 amino acids) is shown in a ternary complex with DNA (purple tube-and-ladder) and an incoming dGTP (PDB: 3GV8) (29). The polι regions are always shown as a yellow cartoon with the lysine located near the functional interface highlighted as a dark blue stick. The lysines that are distal from a functional surface are shown in light blue. K320, whose ubiquitination may destabilize the protein structure, is shown in orange. Some lysine side chains are disordered and are thus modeled as alanine (K51, K83, K283 and K310). *B,* The PIP region of human polι. K421 is near the interface with the green subunit of the trimeric PCNA (the other two PCNA subunits are shown in pink and cyan behind the green subunit) according to the crystal structure (PDB: 2ZVM) (69). *C,* The RIR of human polι is modeled after the crystal structures of human and mouse polκ in a complex with REV1/3/7 (PDB: 4GK5 and 4FJO, respectively). Two lysine residues of the RIR (K549-K550) are conserved, but only one (K550), is near the interface with REV3 and forms a salt bridge with a conserved glutamate of REV1 (E1174 in human REV1). *D,* The UBM1 of human polι is modeled after the NMR structure of mouse UBM1 in a complex with ubiquitin (PDB: 2KWV) (70). K522 is hydrogen bonded with the main chain carbonyl oxygen of L71 in ubiquitin. *E,* UBM2 of human polι in complex with

ubiquitin is shown according to the NMR structure (PDB: 2L0F) (71). K715, the C-terminal residue of polι is near the interface with ubiquitin, while K697 and K704 are distal from ubiquitin.

Table 1: Plasmids used in this study

Plasmid	Description	Source
pJRM46	pCMV6AN-DDK-polι (N-terminal tag)	(13)
pRK7-POLI-3XFLAG	pRK7-3xFLAG-polι (C-terminal tag)	this work
pJRM57	pCMV6AN-DDK-polι_K248A	this work
pJRM48	pCMV6AN-DDK-polι_K522A	this work
pJRM49	pCMV6AN-DDK-polι_K526A	this work
pJRM50	pCMV6AN-DDK-polι_K530A	this work
pJRM51	pCMV6AN-DDK-polι_K549	this work
pJRM52	pCMV6AN-DDK-polι_K704A	this work
pJRM53	pCMV6AN-DDK-polι_K715A	this work
pJRM226	pCMV6AN-DDK-polι_K715R	this work
pJRM54	pCMV6AN-DDK-polι_K704A/K715A	this work
pJRM55	pCMV6AN-DDK-polι_K522A/K526A/ K530A/K549A	this work
pJRM89	pCMV6AN-DDK-polι_K248A/K522A/ K526A/K530A/K549A/K704A/K715A	this work
pJRM106	pCMV6AN-DDK-polι_K237A/K245A/K248A/ K267A/K271A/K522A/K526A/K530A/K549A/ K550A/K704A/K715A	this work
pJRM219	pCMV6AN-DDK-polι_K237R/K245R/K248R/ K267R/K271R/K522R/K526R/K530R/K549R/ K550R/K704R/K715R	this work
pJRM193	pCMV6AN-DDK-polι_K51A/K53A/K72A/ K237A/K245A/K248A/K267A/K271A/K283A/ K309A/K310A/K320A/K522A/K526A/K530A/ K549A/K550A/ K704A/K715A	this work
pJRM192	pCMV6AN-DDK-polι_K51R/K53R/K72R/ K237R/K245R/K248R/K267R/ K271R/K283R/ K309R/K310R/K320R/K522R/K526R/K530R/ K549R/K550R/ K704R/K715R	this work

Table 2: Location of ubiquitination sites in polι and their structural implications[a]

A: Polymerase Domain
K51: located in the finger domain, pointing towards the outside of the protein
K53: located in the finger domain, pointing towards the outside of the protein
K72: located in the finger domain, pointing towards the outside of the protein
K87: located in the finger domain, ~20Å from the incoming nucleotide, may have some effect on catalysis
K138: on the rear side of the protein, when looking at the active site of the polymerase
K203: likely to effect DNA binding and overall structure of the polymerase
K237: likely to effect DNA binding
K245: likely to effect DNA binding
K248: likely to effect DNA binding
K267: on the rear side of the protein, when looking at the active site of the polymerase
K271: ~ 15Å from the upstream DNA duplex, may have some effect on catalysis
K283: on the rear side of the protein, when looking at the active site of the polymerase
K309: may be involved in DNA binding, as it is ~8 Å from the downstream ssDNA
K310: on the same face as DNA binding, but distal from DNA
K320: near D306 and E323 for the structure stability and near the finger domain
K389: on the same face of DNA binding, but distal from DNA

B. PCNA interaction motif
K421: near the PCNA interface

C. UBM1
K508: conserved in mouse (K506) and pointing away from the ubiquitin interface,
K522: conserved in mouse (K520), forming a H-bond with ubiquitin
K526: not conserved in mouse UBM1, N524 of mouse polι points away from the ubiquitin interface
K530: not in the mouse UBM1 structure

D. Rev1 Interacting Region
K549: pointing away from the interface with Rev1
K550: close to the surface of Rev1

E. UBM2
K697: pointing away from ubiquitin
K704: pointing away from ubiquitin
K715: C-terminal residue, not in UBM2 *per se*, but conjugation at this residue would likely position ubiquitin for a non-covalent interaction with UBM2.

[a:] See Figure 11

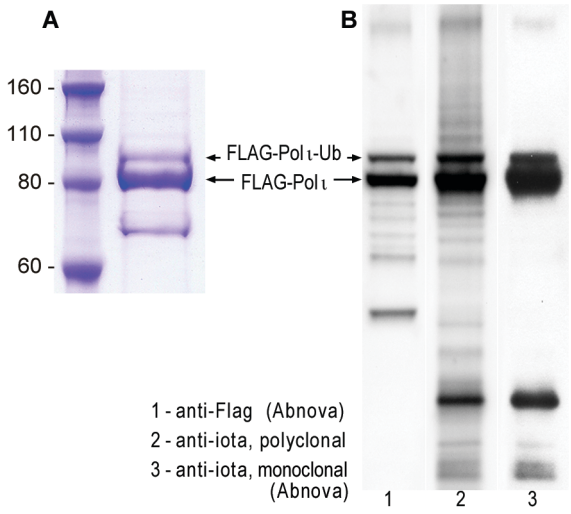

Figure 1

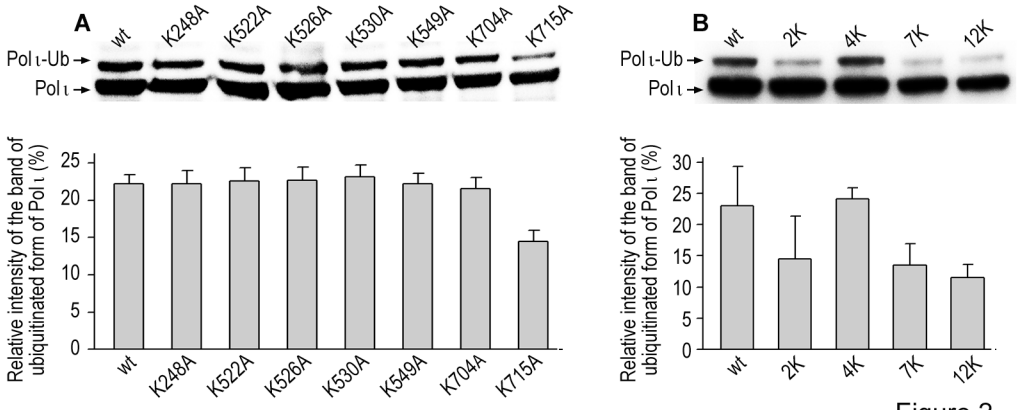

Figure 2

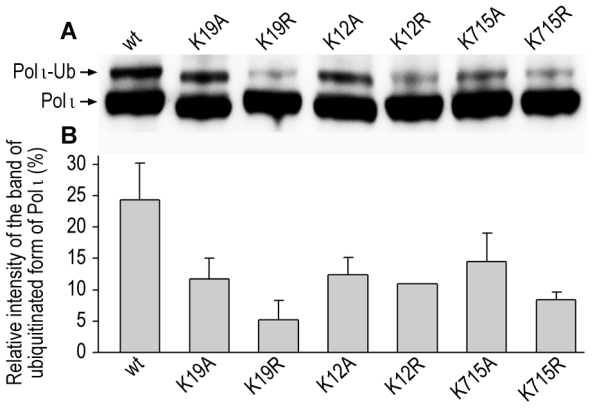

McIntyre et al., Figure 3

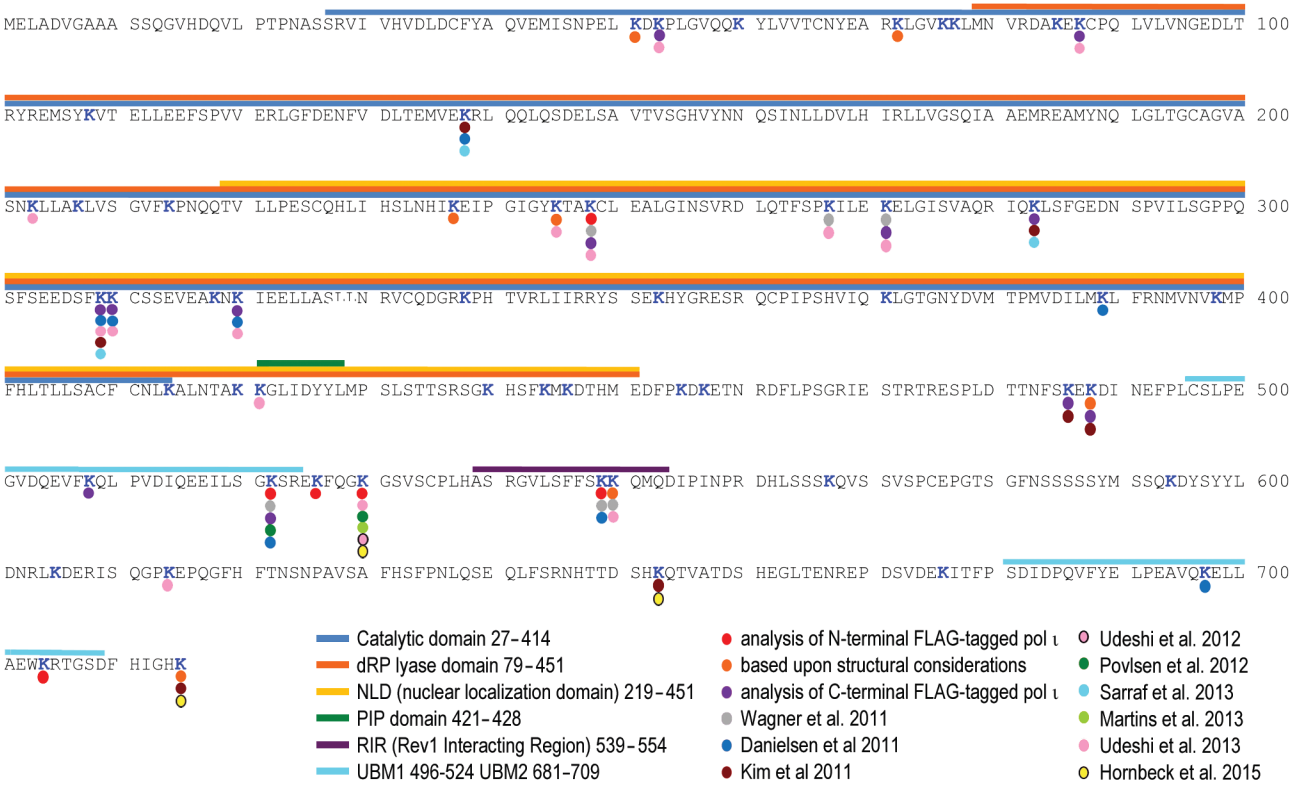

McIntyre et al., Figure 4

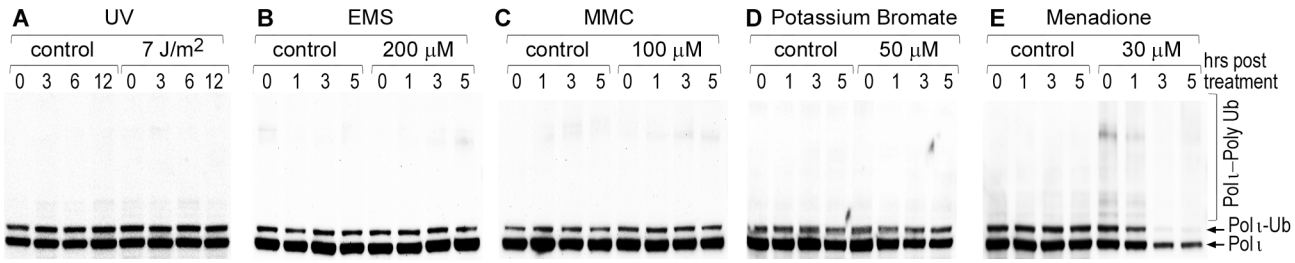

Figure 5

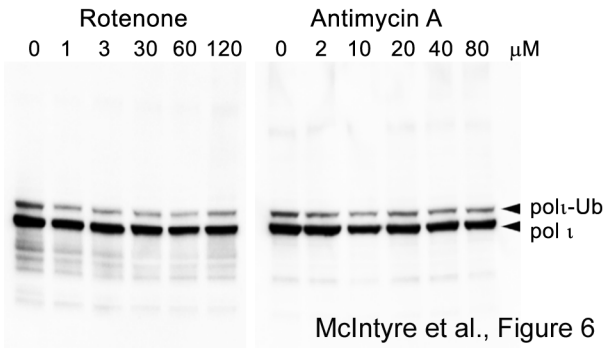

McIntyre et al., Figure 6

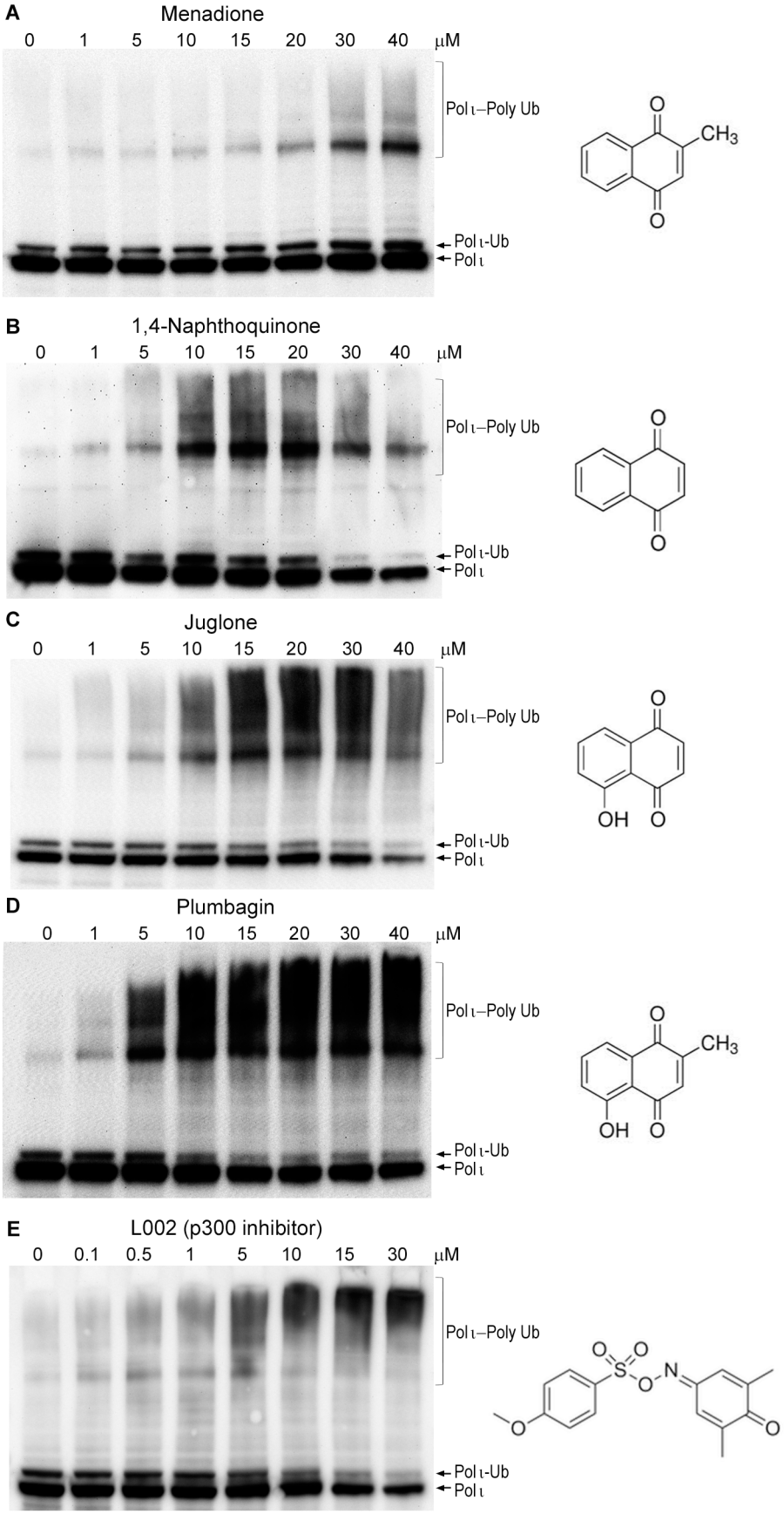

McIntyre et al., Figure 7

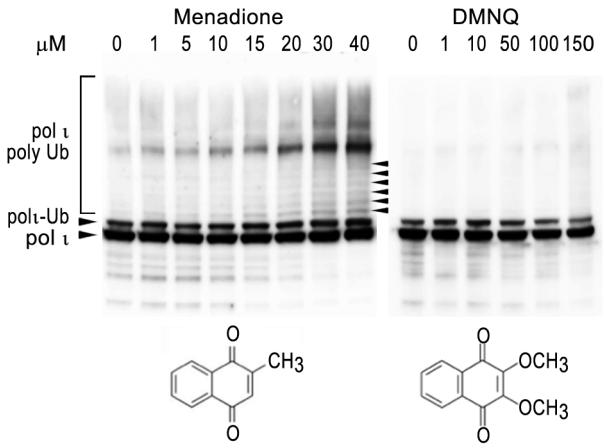

McIntyre et al., Figure 8

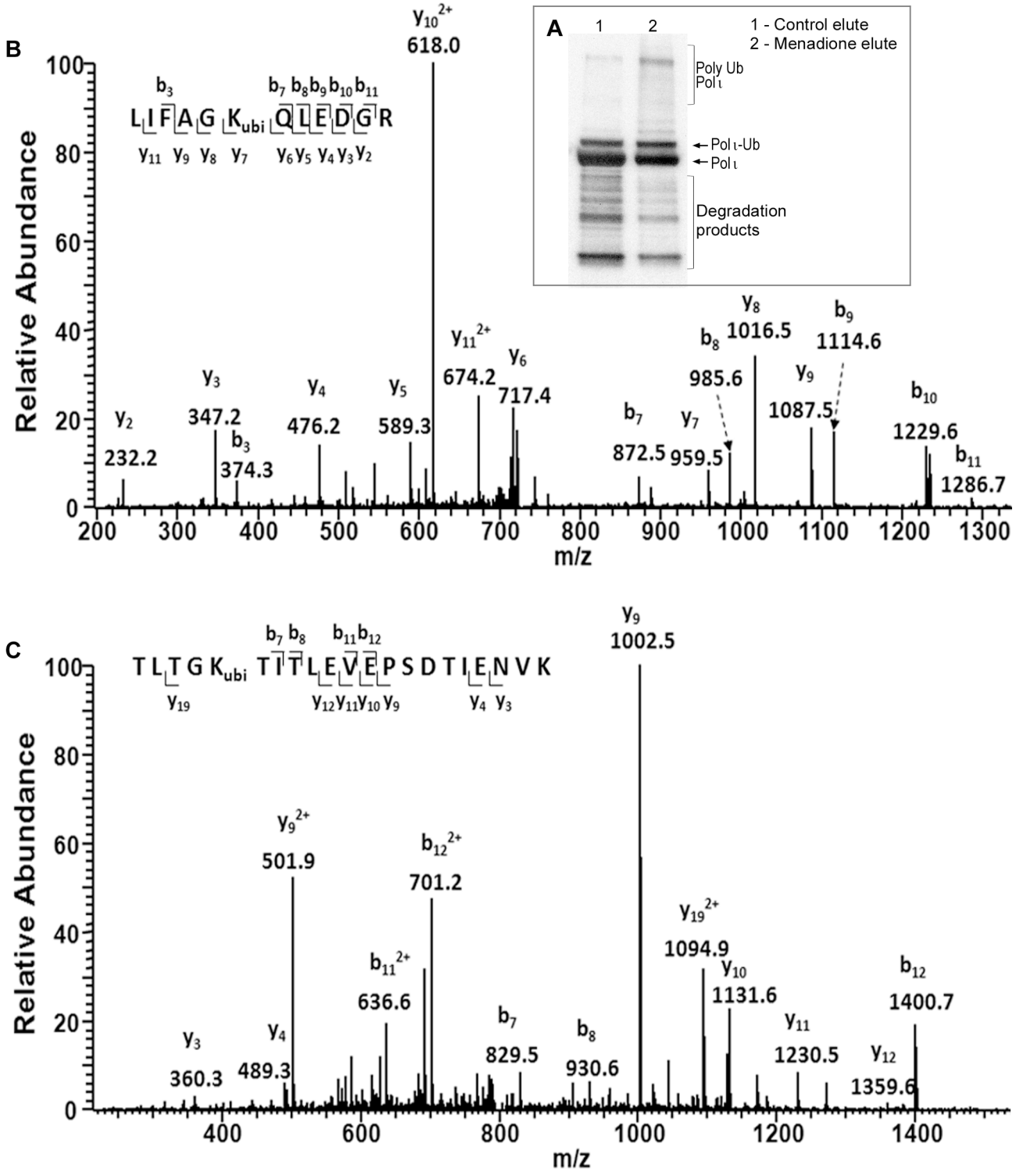

McIntyre et al., Figure 9

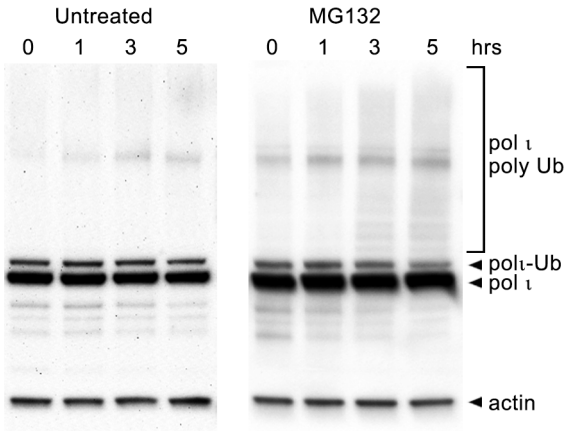

McIntyre et al., Figure 10

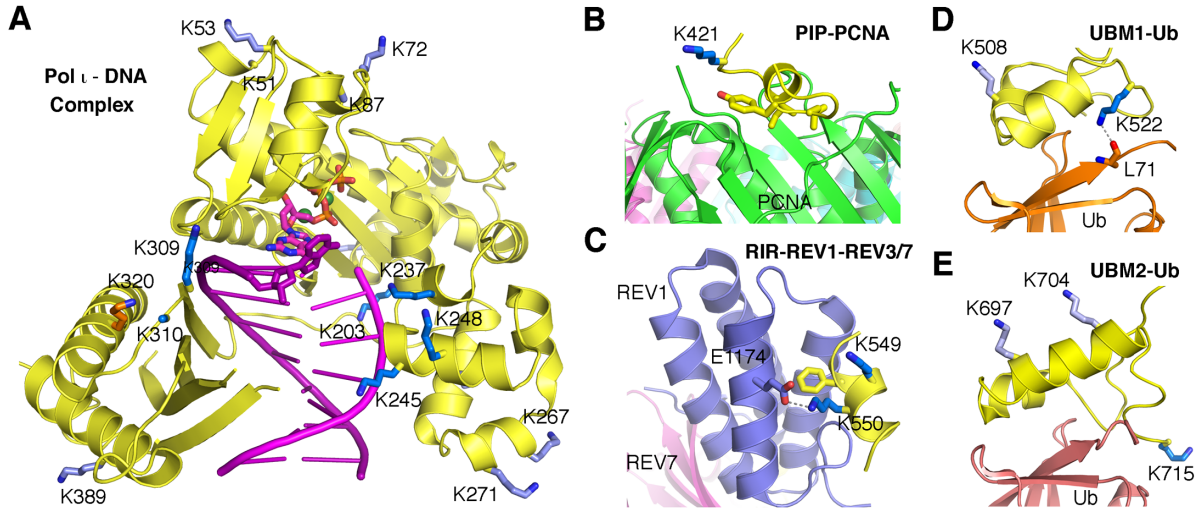

McIntyre et al., Figure 11

DNA and Chromosomes:

Posttranslational Regulation of Human DNA Polymerase ι

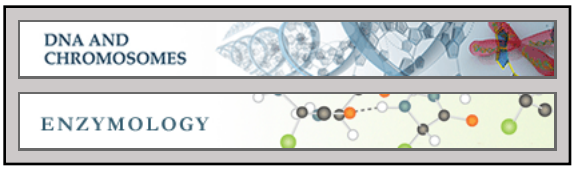

Justyna McIntyre, Mary P. McLenigan, Ekaterina G. Frank, Xiaoxia Dai, Wei Yang, Yinsheng Wang and Roger Woodgate

J. Biol. Chem. published online September 14, 2015

Access the most updated version of this article at doi: 10.1074/jbc.M115.675769